A Harmonic Current Suppression Control Strategy for Droop-Controlled Inverter Connected to the Distorted Grid

Wei, Feng ; Sun, Kai; Guan, Yajuan; Guerrero, Josep M.; Xiao, Xi

Published in:
Proceedings of the 2015 IEEE Energy Conversion Congress and Exposition (ECCE)

DOI (link to publication from Publisher):
10.1109/ECCE.2015.7309734

Publication date:
2015

Document Version
Early version, also known as pre-print

A Harmonic Current Suppression Control Strategy for Droop-Controlled Inverter Connected to the Distorted Grid

Wei Feng[1], Kai Sun[1], Yajuan Guan[2], Josep M. Guerrero[2], Xi Xiao[1]
1) State Key Lab of Power Systems, Department of Electrical Engineering, Tsinghua University, Beijing, China,
2) Department of Energy Technology Department, Aalborg University, Aalborg, Denmark.
fwqqrse@163.com

Abstract—**The grid-feeding voltage controlled inverter (GF-VCI) based on droop control is vulnerable to the harmonic voltages of the utility grid. Because of the equivalent impedance of system is small, the slight distorted grid voltage will result in the harmonic component increasing of GF-VCI output currents. Therefore, the reason of generation of distorted grid-feeding current of GF-VCI under the distorted grid voltage is investigated firstly in this paper. Then, a harmonic grid-feeding current suppression control strategy for GF-VCI is proposed. Two different filters are compared and analysed before being adopted for abstracting the fundamental components of grid voltage. The injected fundamental power is controlled through droop controller, and a hybrid voltage controller of GF-VCI with PI and R regulators in rotary frame is adopted for improving of the tracking capability of the grid harmonic voltage component at the point of common coupling. As a result, the difference of harmonic voltage between PCC and GF-VCI is reduced and the THD_i of grid feeding-currents is decreased. Finally, the proposed control strategy is verified through simulations and experimental results.**

Keywords: Harmonic current; voltage source inverter; droop; microgrid

I. Introduction

NOWADAYS, there is a growing interest in the use of renewable energy sources with the emerging demand and concerns about global warming. One promising power architecture is the microgrid (MG), which usually involves different kinds of energy sources, such as wind or photovoltaic (PV), etc. As a large number of power electronics interfaced distributed generations (DGs) units have been installed in the low-voltage power distribution system [1]-[4], the stability problem is emerging. As a consequence, the performance of DG systems must be improved to meet the grid codes in each country [5].

Though the well-used grid-feeding current controlled inverter (GF-CCI) is easy to control and its equivalent output impedance is almost infinite, the output power of GF-CCI is seriously affected by the irradiation. It means that the power system will suffer more oscillation due to the unsmooth power of inverter when the penetration of GF-CCI or the impedance of transmission line is increasing. Moreover, GF-CCI cannot supply to loads alone under the grid fault condition. For improving the power supplement reliability for sensitive load, the seamless transition between grid-connected and islanded modes is usually required for grid-feeding inverter. Therefore, a mode switch control scheme is proposed in [6] to meet this requirement. However the transient performance between voltage and current control cannot be guaranteed unless additional control strategy is adopted [7].

With the increasing interest of having DGs able to operate in grid-connected and islanded modes with seamless transition, the use of the droop control has been extended widely [8]-[10]. The grid-feeding voltage controlled inverter (GF-VCI) is proposed in [11]. As the outer loop of GF-VCI is voltage controlled, the system can work at islanded mode and supply to loads without additional grid forming unit. In the same time, the power injecting of GF-VCI is controlled by droop controller, which means the inner voltage and current loop of inverter will not be altered when the system work mode switching. The transient response performance is improved.

However, although droop controlled inverter presents high power quality in islanded mode, the GF-VCI is more vulnerable to the harmonic voltages of the grid utility. A slight harmonic of grid voltage may result in high distortion of grid-feeding current at corresponding frequency, because that the equivalent output impedance of GF-VCI is quite small comparing to the GF-CCI. This problem will limit the usage of GF-VCI, especially in the distribution line with high permeation of electronic interfaced DGs. The voltage at the point of common coupling (PCC) may be distorted, because of the increasing of nonlinear loads, alone with the series resonance result from the LCL filter of single inverter, as well as the series and parallel resonance between multiple inverters [12]-[13]. The distorted feeding-current of inverter will further deteriorate the power quality unless additional active power filter (APF) is used.

Therefore, a harmonic grid-feeding current suppression strategy of GF-VCI is discussed in [11], the regular multiple PR controllers are used as voltage controller to deal with harmonic current issue. However, the influence of grid frequency deviation resulting from load disturbance is not considered. Then, in order to avoid the problem of voltage PR controller performance degradation when grid frequency fluctuating, a hybrid voltage and current controlled method (HCM) is proposed in [14], the resonant frequency is adaptive according to grid frequency and power loop. However, the variable parameters controller will make system modeling and stability analysis more difficulty.

According to above-mentioned issue, in order to improve the stability of GF-VCI when grid frequency deviates resulting from the load disturbance, the PI in *dq* frame is adopted as inner voltage controller in this paper. Because the phase used for the Park transform is derived from the estimation of grid by phase lock loop (PLL). The DC voltage reference tracking performance in *dq* frame is guaranteed by PI voltage controller, which means the fundamental component reference in *abc* frame is well tracked by inverter without the influence of frequency deviation.

Then, the reason of generation of distorted grid-feeding current of GF-VCI under the distorted grid voltage is investigated in this paper. A harmonic grid-feeding current suppression control strategy for GF-VCI is proposed. Two different filters are compared and analyzed before being adopted for abstracting the different components of grid voltage. The fundamental injecting power is controlled by droop controller. Multiple resonant regulators are paralleled to the PI voltage controller for improving of the tracking capability of the grid harmonic voltage component at PCC. As a result, the difference of harmonic voltage between PCC and GF-VCI is reduced and the THD_i (The total harmonics distortion of current) of grid feeding-currents is decreased. Finally, the proposed control strategy is verified through simulations and experimental results.

II. Configuration of the Hybrid Microgrid

A. The configuration of hybrid microgrid

In our case, the hybrid MG is consisting of regular power system (such as hydropower plant or diesel generator) to supply the regular local loads, as shown in Fig.1. Each GF-VCI is connected with sensitive local load and powered by energy storing system (ESS) system, which is charged by renewal energy, e.g. PV cell. The DC/DC converter with MPPT algorithm is used for maintaining batteries of ESS and controlling PV penal to output power as much as possible.

The GF-VCI works at the grid-feeding mode and injects dispatched active and reactive to the grid utility when the grid utility is normal. When grid fault happened, the inverter is disconnected from the grid utility and supply to the sensitive local load alone for improving the reliability of power system.

B. The power transfer principle of GF-VCI

The system model of GF-VCI connecting with the grid utility

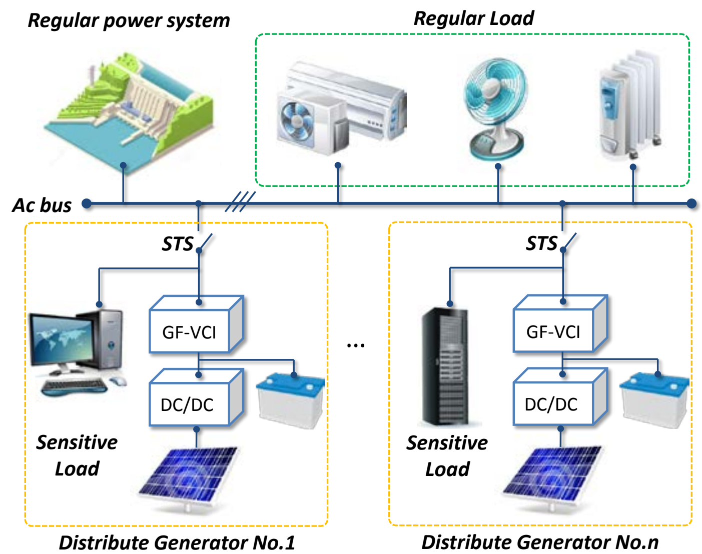

Fig.1. Block diagram of the GD-VCI based MG.

can be simplified to two voltage sources with equivalent impedance and are paralleled with line impedance($sL_{\text{line}} + R_{\text{line}}$), as shown in Fig.2. Where V_{inv} and $\boldsymbol{V}_{\text{grid}}$ represents the voltage vector of GF-VCI and PCC respectively. The vector relationship in Fig.2 is shown in Fig.3.

The active and reactive power transferred from GF-VCI to the grid utility can be calculated from Fig.3, which is shown in following:

$$\begin{cases} P = \dfrac{V_{\text{inv}}V_{\text{grid}}}{Z}\cos(\Delta\phi - \theta) - \dfrac{V_{\text{grid}}{}^2}{Z}\cos(\Delta\phi) \\ Q = \dfrac{V_{\text{inv}}V_{\text{grid}}}{Z}\sin(\Delta\phi - \theta) - \dfrac{V_{\text{grid}}{}^2}{Z}\sin(\Delta\phi) \end{cases} \tag{1}$$

Being P and Q are the transferred active and reactive power between two voltage source, V_{inv} and V_{grid} are amplitude of output voltage of GF-VCI and the grid utility, $\Delta\phi$ represents the phase between voltage vector V_{inv} and $\boldsymbol{V}_{\text{grid}}$. Z and θ are the module and angle of line impedance.

When line impedance is mainly inductive, θ is close to $\pi/2$, The Euq(1) can be simplified to Equ(2), as shown follows:

$$\begin{cases} P = \dfrac{V_{\text{inv}}V_{\text{grid}}}{Z}\sin\Delta\phi \\ Q = \dfrac{V_{\text{inv}}V_{\text{grid}}\cos\Delta\phi - V_{\text{grid}}{}^2}{Z} \end{cases} \tag{2}$$

Therefore, the grid-feeding active and reactive power can be controlled by phase and amplitude difference between the output voltage of GF-VCI and grid voltage at PCC.

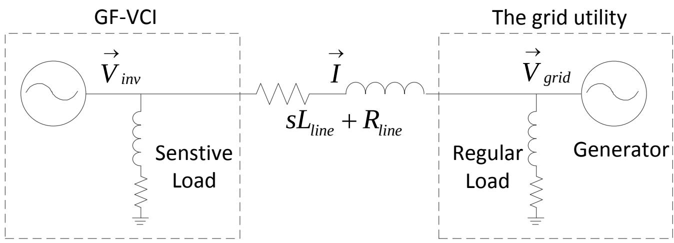

Fig.2. The simplified model of GF-VCI connecting with grid

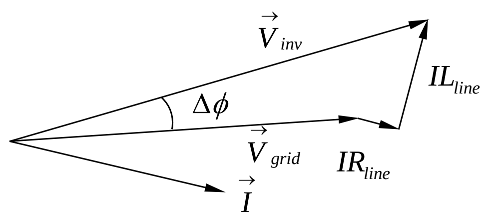

Fig.3. The vector relationship diagram.

III. The Proposed Harmonic Grid-feeding Current Surpression Control strategy

A. The model analysis of GF-VCI

Hypothetically, there is only one harmonic voltage component existing in the grid utility. The equivalent circuit of GF-VCI connecting with the distorted grid is shown in Fig.4 (a), which could be decomposed into fundamental and harmonic component based on linear superposition principle. $G_{\mathrm{v}}(s)$ represents the transfer function of inverter with voltage and current inner controller, as well as LC filter. The equivalent impedance of inverter ($Z_{\mathrm{o}}(s)$) is small when comparing to the line impedance ($Z_{line}(s)$), this is mainly because that the inner controller of inverter is designed to reduce it as small as possible for improving the track performance with voltage reference(v_{ref}). The grid-feeding current of GF-VCI ($i_{grid}(s)$) is resulting from the difference between the output point of inverter and grid connecting point. The different components of model are shown as following:

$$\begin{cases} v_{\mathrm{grid}} = v_{\mathrm{grid\_b}} + v_{\mathrm{grid\_h}} \\ i_{\mathrm{grid}} = i_{\mathrm{base}} + i_{\mathrm{harmonic}} \\ v_{\mathrm{ref}} = v_{\mathrm{ref\_b}} + v_{\mathrm{ref\_h}} \end{cases} \tag{3}$$

Where v_{grid_b} and v_{grid_h}, i_{base} and i_{harmonic}, v_{ref_b} and v_{ref_h} are fundamental and harmonic component of grid voltage and grid-feeding current, as well as the voltage reference of inverter respectively.

Therefore, the modulus of fundamental and harmonic grid-feeding current vector of GF-VCI are derived from Fig.4(b)

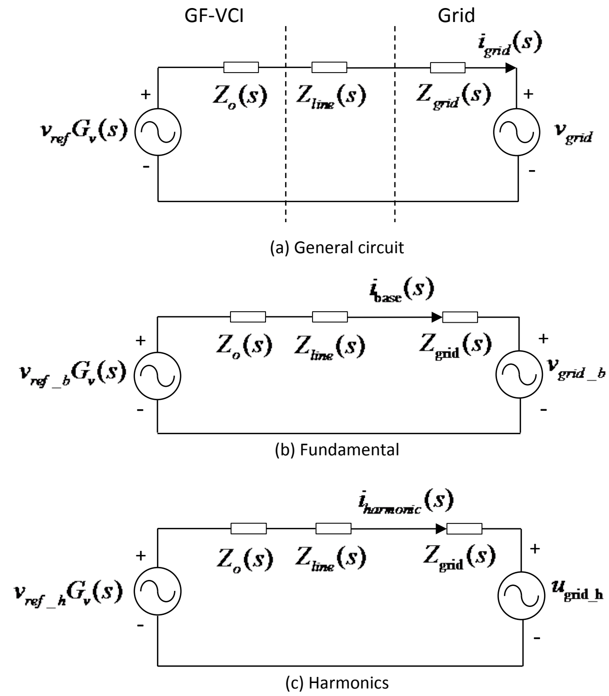

Fig.4. The equivalent circuit diagram of GF-VCI with different component

according to the relationship between complex frequency domain and frequency domain, which are shown as follow:

$$\begin{cases} \left|i_{base}(j\omega_b)\right| = \left|\dfrac{v_{ref\_b}G(j\omega_b) - v_{grid}(j\omega_b)}{Z_o(j\omega_b) + Z_{line}(j\omega_b) + Z_{grid}(j\omega_b)}\right| \\ \left|i_{harmonic}(j\omega_h)\right| = \left|\dfrac{v_{ref\_h}G(j\omega_h) - v_{grid}(j\omega_h)}{Z_o(j\omega_h) + Z_{line}(j\omega_h) + Z_{grid}(j\omega_h)}\right| \end{cases} \tag{4}$$

However, in the conventional control strategy, the inner voltage and current control loop as well as the droop controller of GF-VCI is only designed to guarantee the fundamental voltage control performance in conventional strategy, it be represented as $\left|G_{\mathrm{v}}(j\omega_{\mathrm{h}})\right| << 0dB$ in the amplitude-frequency characteristic analysis of inverter. At same time, there is no harmonic voltage component of grid feeding into inverter voltage reference, in which the phase and amplitude is regulated by droop controller according to the dispatched fundamental power into grid. Therefore, the inverter is equalized to almost shortcut at harmonic frequency when the grid voltage is distorted. Therefore, Equ(5) can be simplified from Equ(4), as shown following:

$$\left|i_{\mathrm{harmonic}}(j\omega_{\mathrm{h}})\right| = \left|-\frac{v_{\mathrm{grid}}(j\omega_{\mathrm{h}})}{Z_o(j\omega_h) + Z_{line}(j\omega_h) + Z_{grid}(j\omega_h)}\right| \tag{5}$$

It is noted that the output fundamental voltage of GF-VCI should be controlled according to fundamental grid-feeding active and reactive power, while the output harmonic voltage of system should be regulated as same with the grid as possible for depressing the harmonic grid-feeding current according to Equ.(4).

B. *The abstracting of foundamental component*

The balanced n^{th} harmonic voltage is presented as trigonometric signal with order of $(n\pm 1)^{th}$ after the Park transform according to its phase sequence. Since PI controller cannot regulate the trigonometric signal without steady error, the output of PLL will be disturbed. Therefore, a filter should be adopted before the estimation of grid phase and voltage amplitude. Two kinds filter are discussed and compared in this paper. The resonant filter is shown as follows:

$$G_{\mathrm{r}}(s)=\frac{ns}{s^2+ns+\omega_{base}^2} \tag{7}$$

Being ω_{base} is set to the fundamental frequency, n is used for altering the attenuation performance. The magnitude-frequency characteristics analysis is shown in Fig.5.

Though the fundamental component can be well decomposed from grid voltage by the resonant filter when grid frequency is fixed to ω_{base} , the phase of filter output will be affected seriously when there is a slight frequency deviation of the grid utility. Therefore, resonant filter in GF-VCI can be used only when connecting with the stiff grid. However, in order to overcome this problem, another kind of notch filter can be adopted in system, as shown follows:

$$G_{\mathrm{notch}}(s)=\frac{s^2+ns+\omega_{har}^2}{s^2+kns+\omega_{har}^2} \tag{8}$$

Where ω_{har} is the frequency of harmonic frequency, k and n are used for adjusting the width of frequency band and the depth of attenuation respectively, which can be seen from the Fig.6.

Though there is only one harmonic component can be filtered by one notch filter, this disadvantage can be easily compensated by the series connection of multiple notch filters, as shown in Equ(8). Moreover, the fundamental component will be not affected when the grid frequency altering. Therefore, the notch filter is applied to weak grid for GF-VCI.

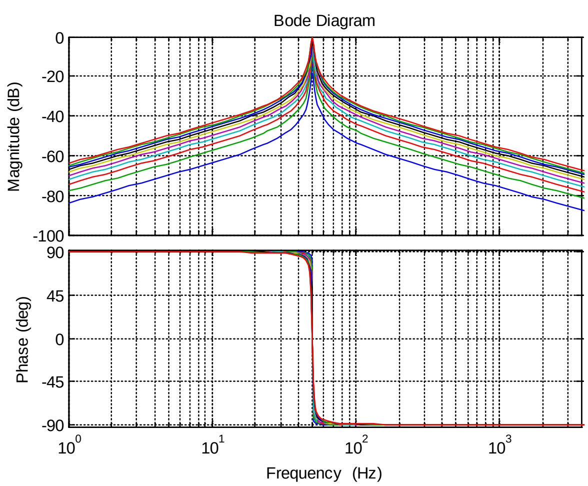

Fig.5. The bode diagram of resonant filter with $n\in[1,10]$

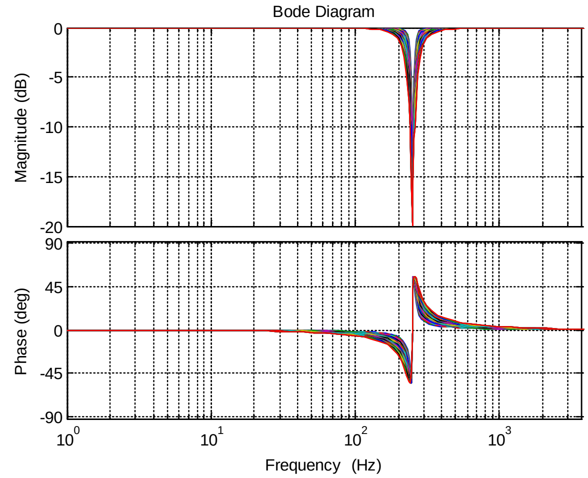

Fig.6. The bode diagram of notch filter with $k=10$ and $n\in[10,40]$

$$\begin{cases} v_{\mathrm{base}}=v_{\mathrm{grid}}\prod_{n=1}^{k}G_{\mathrm{notch},n}(s) \\ v_{\mathrm{harmonic}}=v_{\mathrm{grid}}-v_{\mathrm{base}} \end{cases} \tag{9}$$

C. *The proposed control strategy*

The detailed control scheme of proposed harmonic grid-feeding current suppression control strategy is illustrate in Fig.7. Two PI controllers are adopted in droop loop for controlling the inverter to inject active and reactive power to the grid utility according to the dispatched power reference. A low pass filter (LPF) is used for filter the high frequency component of the output of P/Q calculation for improving the damp performance of system, as shown follows:

$$\begin{cases} \Delta\theta=k_{pP}(P^*-P\dfrac{\omega_c}{s+\omega_c})+k_{iP}\int(P^*-P\dfrac{\omega_c}{s+\omega_c})dt \\ \Delta E=k_{pQ}(Q^*-Q\dfrac{\omega_c}{s+\omega_c})+k_{iQ}\int(Q^*-Q\dfrac{\omega_c}{s+\omega_c})dt \end{cases} \tag{10}$$

Where k_{pP} and k_{iP} , k_{pQ} k_{pp} and k_{iQ} are parameters of active and reactive power controller respectively, ω_c is the time constant of LPF. $\Delta\phi_P$ and ΔE_Q are phase and amplitude increment of fundamental voltage reference.

The final voltage reference of inverter is derived by combining the phase and amplitude of grid voltage detected by PLL (ϕ_g and E_g) and the output of droop controller, as well as the harmonic component of grid voltage, as shown following.

$$\begin{cases} v_{ref\_a}=(\Delta E_Q+E_g)\sin(\Delta\phi_P+\phi_g)+v_{harmonic\_a} \\ v_{ref\_b}=(\Delta E_Q+E_g)\sin(\Delta\phi_P+\phi_g-2\pi/3)+v_{harmonic\_b} \\ v_{ref\_c}=(\Delta E_Q+E_g)\sin(\Delta\phi_P+\phi_g+2\pi/3)+v_{harmonic\_c} \end{cases} \tag{11}$$

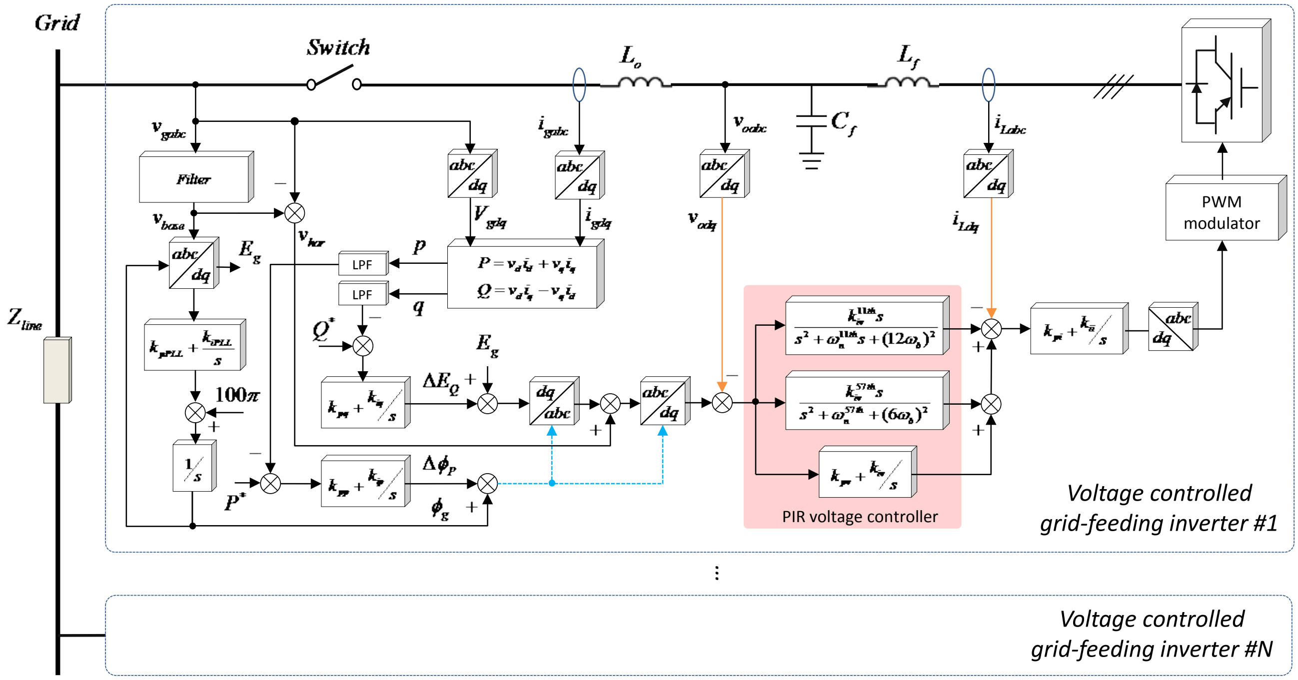

Fig.7. The control scheme of GF-VCI with proposed strategy

In order to improve stability of GF-VCI when connecting with weak grid, in which the load disturbance will result in the deviation of the system frequency. PI controller based on *dq* frame is used to regulate voltage and current of inverter to guarantee the fundamental voltage tracking performance. Moreover, two resonant controllers are adopted in voltage control loop for enhance the harmonic voltage tracking ability of inverter.

As the balanced harmonic voltage component n^{th} are transferred to trigonometric signal with order of $(n \pm 1)^{th}$, the frequency of one resonant controller is set to 300 Hz for 5^{th} negative sequence and 7^{th} positive sequence harmonic components, while another resonant controller is set to 600 Hz for 11^{th} negative sequence and 13^{th} positive sequence harmonic components respectively. Therefore, it can be seen from Fig.8 that the attenuation and phase delay of 0Hz and 300 Hz as well as 600 Hz is zero, which mean the inverter can track voltage reference with no error in steady state at fundamental and 5^{th}, 7^{th}, 11^{th} and 13^{th} harmonic component in *abc* frame.

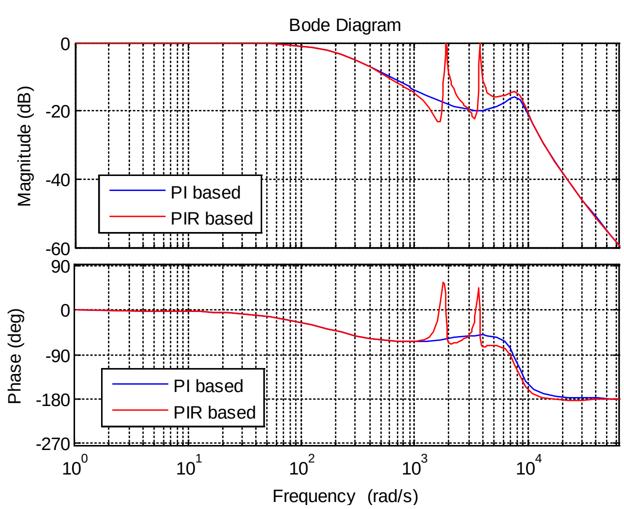

Fig.8. The equivalent circuit diagram of GF-VCI

IV. Simulation and Experimental Results of Proposed Control Strategy

In order to verify the proposed harmonic grid-feeding suppression strategy for GF-VCI, a simulation model is built, which is consisting of the grid utility with harmonic voltage of 5^{th} 7^{th} and 11^{th}, and a 2 kW GF-VCI. The parameters are shown in Tab I. The simulation results are derived according to a scenario in which THD_v of the grid voltage is 1.84%.

TABLE I
THE PARAMETERS OF SIMULATION

Parameter	*Value*	*Parameter*	*Value*
k_{pv}	0.04	k_{iPLL}	1000
k_{iv}	7.24	k_{pP}	5e-4
k_{pi}	0.07	k_{iP}	5e-5
k_{pr}^{1th}	10	k_{dP}	1e-6
ω_n^{1th}	10	k_{pQ}	5e-4
k_{pr}^{57th}	50	k_{iQ}	2e-5
ω_{pr}^{57th}	1	k_{dQ}	1e-6
k_{pr}^{11th}	75	P^*	300 W
ω_n^{11th}	1	Q^*	300 var
k_{pPLL}	14.1	ω_g	50

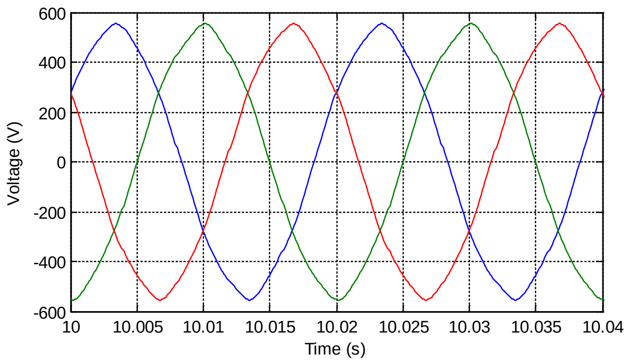

Fig. 9. The distorted grid voltage at PCC

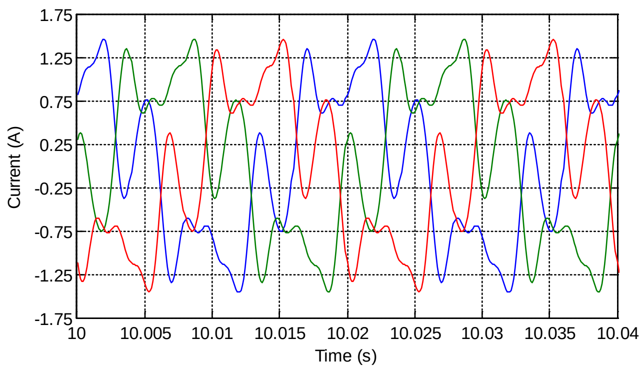

Fig. 10. The grid-feeding current without proposed control strategy

The grid voltage at PCC and grid-feeding current without proposed harmonic suppression control strategy are shown Fig.9 and Fig.10 respectively. It can be seen that the grid-feeding current is highly distorted with THD_i=61.48%, which mainly result from the difference of harmonic voltage between PCC and inverter is not proper controlled. This obviously violates the grid code requirement (THD_i<5%) for grid-feeding inverter. However, when connecting with same distorted voltage, the grid-feeding current of GF-VCI with proposed control strategy is shown in Fig.11. It can be seen that the sinusoidal grid-feeding current is improved. The THD_i of grid-feeding current decreased to 2.21%, which is complying with the requirement of the grid code. The comparing harmonic component analysis of grid-feeding current is shown in Fig.12.

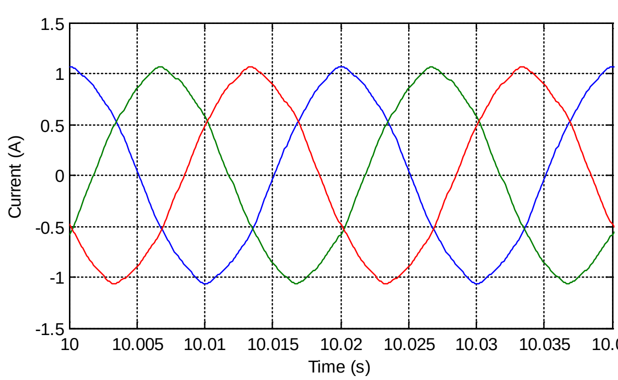

Fig. 11. The grid-feeding current with proposed control strategy

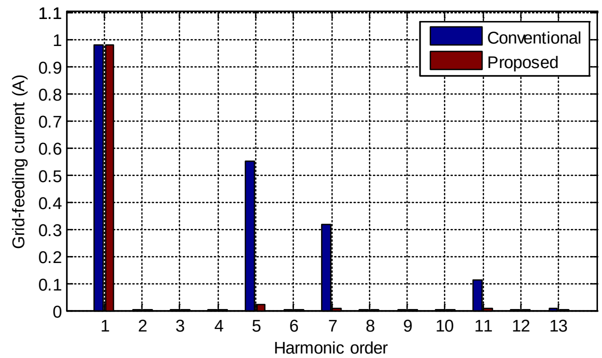

Fig. 12. The comparing harmonic analysis of grid-feeding current

The effectiveness of the proposed harmonic grid-feeding current suppression control strategy is also evaluated through a scale-down laboratory prototype. The experimental setup consists of two Danfoss 2.2 kW inverters, a dSPASE1006 control board, LCL filters, LEM sensors and two resistive loads, as shown in Fig.5. One of the inverter is used to simulate the distorted grid with different harmonic voltage components. The other employs the droop controller and proposed control strategy to simulate the GF-VCI. The electrical parameters of setup are listed in and II.

TABLE III
SYSTEM PARAMETERS OF SETUP

Parameter	***Value***	***Parameter***	***Value***
V_{dc}	650V	$Load_2$	670 W
V_{ac}	230V	$P*$	300 W
L_f	1.8e-3 H	$Q*$	0 var
C_f	9e-6 F	$Vref^{5th}$	5 V
L_o	1.8e-3 H	$Vref^{7th}$	5 V
$Load_1$	340 W		

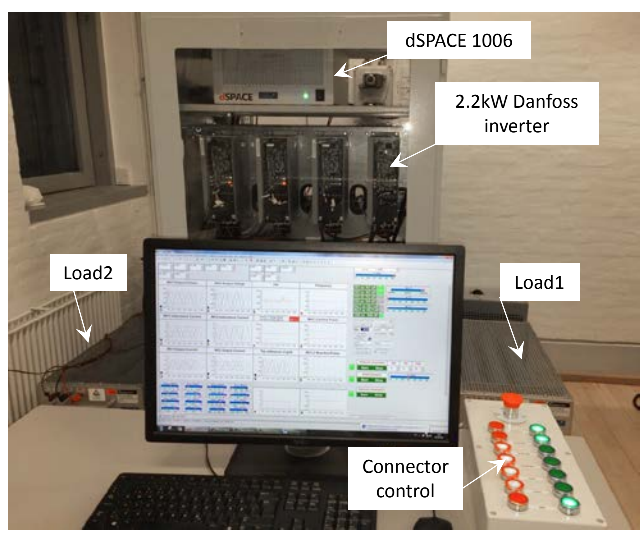

Fig. 13. The scale-down experimental setup.

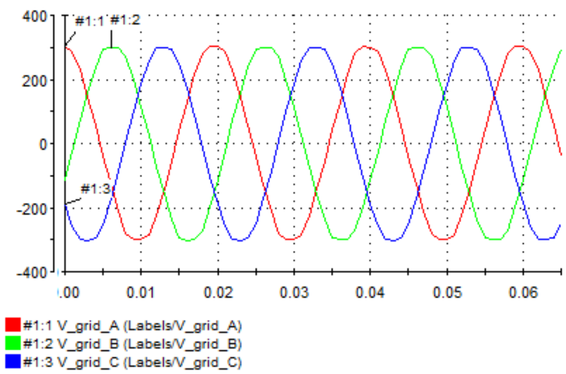

Fig. 14. Distorted voltage waveform of grid simulator

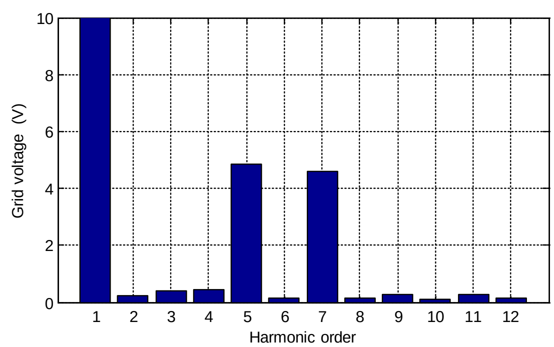

Fig. 15. The harmonic analysis of grid voltage

The output voltage of grid simulator and its harmonic analysis are shown in Fig.14 and Fig.15 respectively. It can be seen that the grid is distorted with 5th and 7th harmonic voltage and the corresponding harmonic component is 4.8V and 4.2V.

When GF-VCI is connecting with distorted voltage, the grid-feeding current of system without proposed control strategy is shown in Fig.16. As the poor harmonic voltage tracking performance of GF-VCI with conventional control strategy, and there is no corresponding harmonic voltage components in the reference of inverter. The harmonic components of grid-feeding current are increased, resulting from the voltage difference between output of GF-VCI and the grid simulator is not suppressed properly.

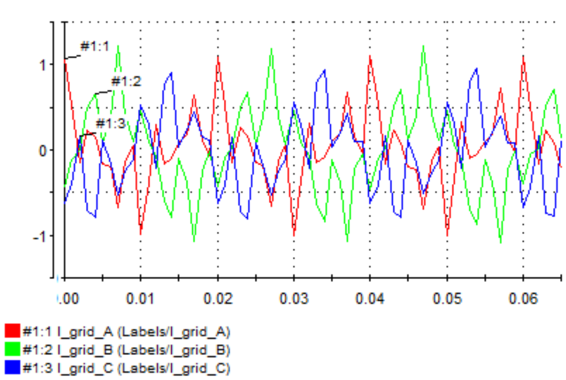

Fig. 16. The grid-feeding current of GF-VCI without the proposed strategy

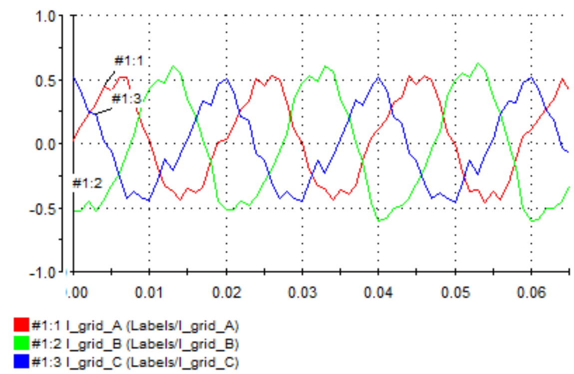

Fig. 17. The grid-feeding current of GF-VCI with the proposed strategy

In the same way, the grid-injecting current of GF-VCI with proposed harmonic grid-feeding current suppression control strategy is shown in Fig.17. It is note that the THD$_i$ of grid-feeding current is decreased considerably, it is because that there is almost only fundamental voltage phase and amplitude difference between inverter and PCC.

The comparing harmonic analysis of grid-feeding current of experiments is presented in Fig.18. The 5th and 7th harmonic components of current are 0.34A and 0.31A respectively when conventional control strategy is adopted. However, the corresponding harmonic component is reduced to 0.03A and 0.035A by the proposed strategy.

The harmonic voltage disturbance of grid simulator is used for testing the dynamic response of proposed control strategy. The 5th and 7th harmonic voltage disturbance

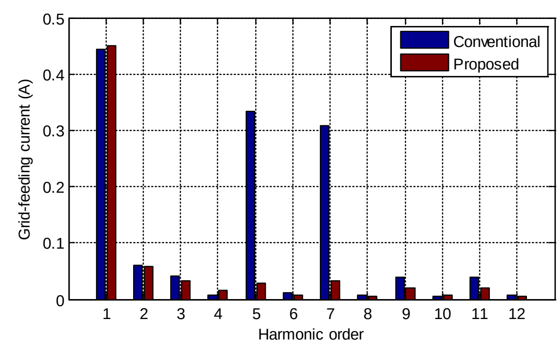

Fig. 18. Harmonic analysis of grid-feeding current

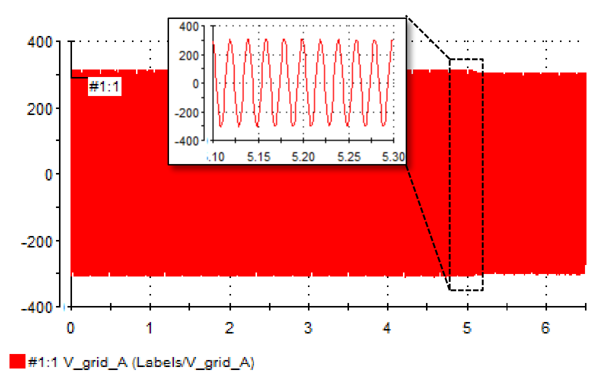

Fig. 19. Harmonic voltage disturbance

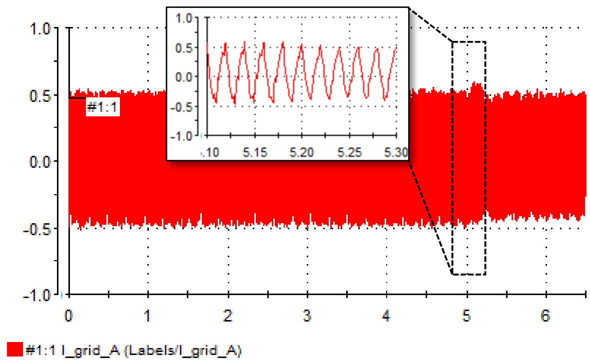

Fig. 20. The dynamic response of proposed control strategy

happened around 5s, as shown in Fig.19. The grid-feeding current of GF-VCI with proposed control strategy is depicted in Fig.20. It can be seen that the grid-feeding current gets distorted immediately after voltage harmonic disturbance happened, however the proposed controller starts to work after round 0.2s and the total dynamic response is about 0.5s.

V. Conclusion

In this paper, a harmonic grid-feeding current suppression control strategy is proposed for the droop-controlled inverter under distorted grid. The equivalent model is established for investigating the generation of the harmonic grid-feeding current of GF-VCI. Two kinds filter are analyzed and compared before being used for decomposing the different components of grid voltage. The injecting fundamental active and reactive power is controlled by modulating the phase and amplitude of voltage fundamental component of inverter based on the grid utility. A compound PIR voltage controller is adopted into the voltage loop of inverter to enhance the harmonic voltage tracking ability. Therefore, the difference of harmonic voltage between inverter and PCC is reduced and power quality of grid-feeding current is improved. The Simulation and experimental results show the effectiveness of the proposed approach.

Acknowledgement

The authors would like to appreciate the supports by National Natural Science Foundation of China (51177083), National International Science & Technology Cooperation Project (2014DFG62610), and State Key Lab of Power Systems (SKLD14M01), Tsinghua University.

References

[1] R. Lasseter, A. Akhil, C. Marnay, J. Stevens, et al, "The certs microgrid concept - white paper on integration of distributed energy resources," Technical Report, U.S. Department of Energy, 2002.

[2] C. K. Sao and P. W. Lehn, "Autonomous load sharing of voltage source converters," *IEEE Trans. Power Del.*, vol. 20, no. 2, pp. 1009–1016, 2005.

[3] Guerrero, J.M., Chandorkar, M., Lee, T., Loh, P.C., "Advanced Control Architectures for Intelligent Microgrids—Part I: Decentralized and Hierarchical Control," Industrial Electronics, IEEE Transactions on, vol.60, no.4, pp.1254-1262, April 2013.

[4] Yu Xiao, KhambadkoneA M, Wang Huan, et al. "Control of Parallel-Connected power converters for Low-Voltage microgrid—part i: a hybrid control architecture," Power Electronics, IEEE Transactions on, vol.25, no.12, pp., 2962-2970. 2010.

[5] Kyoung-Jun Lee , Jong-Pil Lee, Dongsul Shin, "A Novel Grid Synchronization PLL Method Based on Adaptive Low-Pass Notch Filter for Grid-Connected PCS," Industrial Electronics, IEEE Transactions on, vol.61, no.1, pp.292-301, April 2014.

[6] Zhiqiang Guo, Deshang Sha, Xiaozhong Liao, "Voltage magnitude and frequency control of three-phase voltage source inverter for seamless transfer," IET. Power Electronics, vol. 7, no. 1, pp. 200–208, 2014.

[7] Tai-Sik Hwang, Sung-Yeul ParkA, "Seamless Control Strategy of a Distributed Generation Inverter for the Critical Load Safety Under Strict Grid Disturbances, " Power Electronics, IEEE Transactions on, vol.28, no.10, pp., 4780-4790. 2012.

[8] C. T. Lee, C. C. Chu and P. T. Cheng, "A new droop control method for the autonomous operation of distributed energy resource interface converters," *IEEE Trans. Power Electron.*, vol. 28, no. 4, pp. 1980-1993, 2013.

[9] Y. W. Li and C. N. Kao, "An accurate power control strategy for power-electronics-interfaced distributed generation units operating in a low-voltage multibus microgrid," IEEE Trans. Power Electron., vol. 24, no. 12, pp. 2977–2988, 2009.

[10] J. C. Vasquez, J. M. Guerrero, A. Luna, et al, "Adaptive droop control applied to voltage-source inverters operation in grid-connected and islanded modes," *IEEE Trans. Ind. Electron.*, vol. 56, no. 10, pp. 4088-4096, 2009.

[11] J. He, Y. W. Li, and S. Munir, "A flexible harmonic control approach through voltage-controlled DG-grid interfacing converters," IEEE Trans. Ind. Electron., vol. 59, no. 1, pp. 444–455, Jan. 2012.

[12] Jinwei He, Yun Wei Li, Bosnjak, D., Harris, B, "Investigation and resonances damping of multiple PV inverters," IEEE APEC2012, Orlando, 2012.

[13] Jinwei He, Yun Wei Li, Bosnjak, D. "Investigation and Active Damping of Multiple Resonances in a Parallel-Inverter-Based Microgrid," Power Electronics, IEEE Transactions on, vol.28, no.1, pp., 234-246. 2014.

[14] Jinwei He, YunWei Li, Frede Blaabjerg, "Flexible Microgrid Power Quality Enhancement Using Adaptive Hybrid Voltage and Current Controller," Industrial Electronics, IEEE Transactions on, vol.61, no6, pp.2784-2794, April 2014.